ELSEVIER

Journal of Organometallic Chemistry 545–546 (1997) 369–379

Journal of Organometallic Chemistry

Preparation and electrochemical reactions of nickel(II) complexes containing isocyanide and mono- or di-phosphines

Yasuhiro Yamamoto *, Hiroyuki Takahata, Fumie Takei

Department of Chemistry, Faculty of Science, Toho University, Funabashi, Chiba 274, Japan

Received 26 March 1997; received in revised form 14 May 1997

Abstract

Reactions of *cis*-$NiCl_2$(diphos) (diphos = $PPh_2(CH_2)_nPPh_2$: $n = 2$ (dppe); $n = 3$ (dppp)) with isocyanide in the presence of NH_4PF_6 gave [NiCl(diphos)(XylNC)$_2$](PF_6) (**1**, **2**) or [Ni(diphos)(RNC)$_3$](PF_6)$_2$ (**3**, **4**) (R = 2,6-$Me_2C_6H_3$ (Xyl), 2,4,6-$Me_3C_6H_2$ (Mes)). Similar reactions of $NiCl_2(PPh_3)_2$ with xylyl isocyanide gave [$NiCl(PPh_3)_2$(XylNC)$_2$](PF_6) **5** and [$Ni(PPh_3)_2$(XylNC)$_3$](PF_6)$_2$ **6**. The structures of these five-coordinated complexes were confirmed to be square-pyramidal by X-ray analyses: [NiCl(dppp)(XylNC)$_2$](PF_6) · CH_2Cl_2 **2a**, $a = 13.345(2)$ Å, $b = 10.984(2)$ Å, $c = 33.082(4)$ Å, $\beta = 97.13(1)°$, $V = 4812(3)$ Å^3, monoclinic, $P2_1/c$, $z = 4$, $R = 0.064$; [Ni(dppe)(MesNC)$_3$](PF_6)$_2$ **3b**, $a = 12.763(3)$ Å, $b = 13.110(3)$ Å, $c = 17.114(3)$ Å, $\beta = 102.55(2)°$, $V = 2795(2)$ Å^3, monoclinic, Pn, $z = 2$, $R = 0.051$; [$NiCl(PPh_3)_2$(XylNC)$_2$](PF_6) **5a**, $a = 13.768(5)$ Å, $b = 17.23(1)$ Å, $c = 11.063(6)$ Å, $\alpha = 98.86(4)°$, $\beta = 95.97(4)°$, $\gamma = 75.48(3)°$, $V = 2504(2)$ Å^3, triclinic, P1, $z = 2$, $R = 0.063$. The CV's of these complexes showed to be quasi-reversible with two-electron transfer. The potentials of complexes (**1**, **2**, **5**) shifted to more negative region than those of the corresponding **3**, **4**, and **6**, respectively. There exists an equilibrium between **1** and **3** in the presence of isocyanide on the basis of the $E_{1/2}$ potentials, but no equilibrium between **2** and **4**. Complex **5** was completely converted to **6** in the presence of xylyl isocyanide. These complexes were not influenced for excess diphosphine. © 1997 Elsevier Science S.A.

1. Introduction

The electrochemical reactions of organometallic compounds are very important as the preparative methods of new organometallic compounds and also as valuable sources of mechanistic informations. We have continued to report systematic electrochemical studies of platinum and palladium isocyanide complexes such as $MCl_2(RNC)_2$, $[M(RNC)_4]^{2+}$ and $[M(RNC)_2(diphos)]^{2+}$ (M = Pt, Pd; diphos = $Ph_2P(CH_2)_nPPh_2$) [1–10]. Recently, we described that the electrochemical reductions of $NiX_2(RNC)_2$ (X = Cl, Br, I) showed unusual behaviors depending on the different electrode materials. When a hanging-mercury-drop electrode was used, the chemical reaction of $NiX_2(RNC)_2$ with Hg atom occurred to lead to formation of the Hg–Ni donor–acceptor complex before the electrochemical reaction proceeds [11,12]. However, the use of a platinum electrode as a working one showed a usual electroreductive behavior of $NiX_2(RNC)_2$. In comparison with the nickel isocyanide complexes [11,12], and platinum and palladium complexes containing isocyanide and phosphine ligands [1–10], we described the preparation and electrochemical reactions of the five coordinated nickel complexes with isocyanide and phosphine.

2. Experimental

2.1. Materials

Dichloromethane and acetonitrile were purified by distillation over CaH_2, and acetone was distilled. Isocyanides [13], *cis*-$NiCl_2$(dppe) [14–16], and *cis*-$NiCl_2$(dppp) [15] were prepared according to the literature methods. Bis(diphenylphosphino)ethane (dppe) and bis(diphenylphosphino)propane (dppp) are commercially available. The infrared and electronic absorption spectra were measured on FT/IR-5300 and U-best 30 spectrometers, respectively. NMR spectroscopy was carried out on a Bruker AC250. ^{1}H chemical shifts were

* Corresponding author.

PII S0022-328X(97)00343-4

measured against Me_4Si using solvent resonances as standard locks. Cyclic voltammograms were recorded using a HUSO 956B potentiostat and a HUSO 321 potential scanning unit. The electrochemical procedures were carried out according to literature methods [11,12]. Working electrode used was a Pt disk electrode (0.02 cm^2). A Pt wire was used as a counter electrode. The reference electrode was $Ag/AgNO_3$ (0.1 mol dm^{-3})–[$^nBu_4N$](ClO_4)/MeCN (0.1 mol dm^{-3}) system, whose potential was determined relative to a ferrocene(Fc)/ferrocenium(Fc^+) (1×10^{-3} mol dm^{-3}) couple at the end of each experiment. Electrochemical measurements were carried out in a ca. 0.1 M (1 M = 1 mol dm^{-3}) solution of [$^nBu_4N$](ClO_4)MeCN/CH_2Cl_2 (9:1) under a nitrogen atmosphere at room temperature after the solution was deaerated by bubbling with nitrogen. All potentials are indicated vs. Fc/Fc^+.

2.2. Preparation of [NiCl(dppe)(XylNC)$_2$](PF$_6$) (1a)

Xylyl isocyanide (0.214 g, 1.63 mmol) and NH_4PF_6 (0.139 g, 0.85 mmol) in a mixture of CH_2Cl_2 (20 cm^3) and acetone (20 cm^3) were added to a solution of *cis*-$NiCl_2$(dppe) (0.4 g, 0.76 mmol) in CH_2Cl_2 (15 cm^3) and acetone (5 cm^3). After stirred for 2 h at room temperature, the solvent was removed under reduced pressure and the residue was extracted with CH_2Cl_2, followed by recrystallization from CH_2Cl_2 and diethyl ether to give orange crystals of the title compound (0.479 g, 70%). IR (nujol): 2182, 2170(sh) (N ≡ C), 837 (PF_6) cm^{-1}. Electronic spectrum (CH_2Cl_2): λ_{max} 395 (log ε 3.28), 285 (4.48) nm. ^1H NMR ($CDCl_3$): δ 2.04 (s, Me, 12H), 3.18 (d, J_{PH} = 13.8 Hz, CH_2, 4H), 6.95–7.73 (m, Ph, 26H) ppm. $^{31}P\{^1H\}$ NMR ($CDCl_3$): δ 70.1 (s, 2P), −143.9 (sep, J_{PF} = 709 Hz, PF_6) ppm. Anal. Calcd for $C_{44}H_{42}N_2ClF_6P_3Ni$: C, 58.73; H, 4.70; N, 3.11. Found: C, 58.45; H, 4.71; N, 3.06.

The dppp complex [NiCl(dppp)(XylNC)$_2$](PF$_6$)$_2$ · CH_2Cl_2 **2a** (69%) was prepared by the procedure similar to that described above. IR (nujol): 2178, 2164 (N ≡ C), 837 (PF_6) cm^{-1}. Electronic spectrum (CH_2Cl_2): λ_{max} 393 (3.17), 281 (4.36) nm. ^1H NMR ($CDCl_3$): δ 2.04 (s, Me, 12H), 2.50 (b, CH_2), 3.21 (br, CH_2), 5.27 (s, CH_2Cl_2), 6.87–7.68 (m, Ph) ppm. $^{31}P\{^1H\}$ NMR ($CDCl_3$): δ 4.3 (s, 2P), −144.5 (sep, J_{PF} = 710 Hz, PF_6) ppm. Anal. Calcd for $C_{46}H_{46}N_2Cl_3F_6P_3Ni$: C, 56.50; H, 4.69; N, 2.88. Found: C, 56.35; H, 4.90; N, 2.85.

2.3. Preparation of [NiBr(dppe)(XylNC)$_2$](PF$_6$) (1b)

To a solution of [NiCl(dppe)(XylNC)$_2$](PF$_6$) (**1a**) (0.70 g, 0.78 mmol) in CH_2Cl_2 (15 cm^3) and H_2O (5 cm^3) was KBr (0.462 g, 3.88 mmol) in H_2O (5 cm^3) added at room temperature. After 2 h, the organic layer was dried over Na_2SO_4. The solvent was removed under reduced pressure and the residue was recrystallized from CH_2Cl_2 and diethyl ether to give reddish brown crystals of the title compound (**1b**) (0.633 g, 86%). IR (nujol): 2172, 2168 (N ≡ C), 839 (PF_6) cm^{-1}. Electronic spectrum (CH_2Cl_2): λ_{max} 402 (3.18), 283 (4.43) nm. ^1H NMR ($CDCl_3$): δ 2.06 (s, Me, 12H), 3.19 (d, J_{PH} = 13.9 Hz, CH_2, 4H), 6.94–7.74 (m, Ph, 26H) ppm. $^{31}P\{^1H\}$ NMR ($CDCl_3$): δ 79.3 (s, 2P), −143.8 (sep, J_{PF} = 709 Hz, PF_6) ppm. Anal. Calcd for $C_{44}H_{42}N_2BrF_6P_3Ni$: C, 55.97; H, 4.48; N, 2.97. Found: C, 55.65; H, 4.40; N, 2.87.

Iodide complex [NiI(dppe)(XylNC)$_2$](PF$_6$) · $1/2CH_2Cl_2$ (**1c**) (86%) was also obtained by the metathesis reaction of **1a** with KI. IR (nujol): 2173, 2167 (N ≡ C), 839 (PF_6) cm^{-1}. Electronic spectrum (CH_2Cl_2): λ_{max} 455 (log ε 2.87), 285 (4.45), 248 (4.54) nm. ^1H NMR ($CDCl_3$): δ 2.13 (s, Me, 12H), 3.19 (d, J_{PH} = 13.8 Hz, CH_2, 4H), 6.94–7.73 (m, Ph, 26H) ppm. $^{31}P\{^1H\}$ NMR ($CDCl_3$): δ 68.5 (s, 2P), −144.4 (sep, J_{PF} = 710 Hz, PF_6) ppm. Anal. Calcd for $C_{44.5}H_{43}N_2ClIF_6P_3Ni$: C, 51.70; H, 4.19; N, 2.71. Found: C, 51.52; H, 4.04; N, 2.53.

The bromide and iodide complexes of dppp were prepared according to the procedure described above. [NiBr(dppp)(XylNC)$_2$](PF$_6$) · $2/3CH_2Cl_2$ (**2b**) (81%): IR (nujol): 2180(sh), 2166 (N ≡ C), 837 (PF_6) cm^{-1}. Electronic spectrum (CH_2Cl_2): λ_{max} 408 (2.97), 281 (4.25) nm. ^1H NMR ($CDCl_3$): δ 2.06 (s, Me, 12H), 2.56 (b, CH_2), 3.36 (b, CH_2), 5.27 (s, CH_2Cl_2), 6.86–7.69 (m, Ph, 26H) ppm. $^{31}P\{^1H\}$ NMR ($CDCl_3$): δ 3.4 (s, 2P), −144.4 (sep, J_{PF} = 710 Hz, PF_6) ppm. Anal. Calcd for $C_{45}H_{44}N_2BrF_6P_3Ni \cdot 2/3CH_2Cl_2$: C, 54.01; H, 4.63; N, 2.76. Found: C, 54.18; H, 4.63; N, 2.62. [NiI(dppp)(XylNC)$_2$](PF$_6$) · $2/3CH_2Cl_2$ **2c** (85%): IR (nujol): 2180(sh), 2164 (N ≡ C), 835 (PF_6) cm^{-1}. Electronic spectrum (CH_2Cl_2): λ_{max} 451 (3.02), 276(sh), 247 (4.58) nm. ^1H NMR ($CDCl_3$): δ 2.10 (s, Me, 12H), 2.56 (b, CH_2, 6H), 3.35 (b, CH_2), 5.28 (s, CH_2Cl_2), 6.87–7.68 (m, Ph, 26H) ppm. $^{31}P\{^1H\}$ NMR ($CDCl_3$): δ 1.7 (s, 2P), −144.4 (sep. J_{PF} = 709 Hz) ppm. Anal. Calcd for $C_{45}H_{44}N_2IF_6P_3Ni \cdot 2/3CH_2Cl_2$: C, 51.63; H, 4.27; N, 2.67. Found: C, 51.53; H, 4.39; N, 2.53.

2.4. Preparation of [Ni(dppe)(XylNC)$_3$] (PF$_6$)$_2$ · 1/2CH$_2$Cl$_2$ (3a · 1/2CH$_2$Cl$_2$)

Xylyl isocyanide (0.34 g, 2.59 mmol) and NH_4PF_6 (0.598 g, 3.67 mmol) in CH_2Cl_2 (20 cm^3) and acetone (20 cm^3) was added to *cis*-$NiCl_2$(dppe) (0.40 g, 0.76 mmol) in CH_2Cl_2 (15 cm^3) and acetone (5 cm^3). After stirred for 2 h, the solvent was removed to dryness and the residue was extracted with CH_2Cl_2. Crystallization from CH_2Cl_2 and diethyl ether gave orange crystals (0.581 g, 65%) of the title complex. IR (nujol): 2191, 2172 (N ≡ C), 839 (PF_6) cm^{-1}. Electronic spectrum (CH_2Cl_2): λ_{max} 341(sh), 251 (4.70) nm. ^1H NMR

($CDCl_3$): δ 2.04 (s, Me, 18H), 3.18 (d, CH_2, J_{PH} = 22.6 Hz), 5.30 (s, CH_2Cl_2), 7.03–7.86 (m, Ph) ppm. $^{31}P\{^1H\}$ NMR ($CDCl_3$): δ 79.8 (s, 2P), −144.4 (sep. J_{PF} = 709 Hz) ppm. Anal. Calcd for $C_{53.5}H_{52}N_3ClF_{12}P_4Ni$: C, 54.32; H, 4.43; N, 3.55. Found: C, 54.58; H, 4.42; N, 3.42.

The mesityl isocyanide and dppp complexes were prepared according to the procedure described above. $[Ni(dppe)(MesNC)_3](PF_6)_2$ (**3b**) (orange, 87%): IR (nujol): 2193, 2183, 2168 (N ≡ C), 841 (PF_6) cm^{-1}. Electronic spectrum (CH_2Cl_2): λ_{max} 360(sh), 255 (4.01) nm. ^1H NMR ($CDCl_3$): δ 1.98 (s, *o*-Me), 2.27 (s, *p*-Me), 3.17 (d, J_{PH} = 22.7 Hz), 6.83 (s, *m*-H), 7.50–7.90 (m, Ph) ppm. Anal. Calcd for $C_{56}H_{57}N_3F_{12}P_4Ni$: C, 56.87; H, 4.86; N, 3.55. Found: C, 56.50; H, 4.85; N, 3.41.

$[Ni(dppp)(XylNC)_3](PF_6)_2$ (**4**) (orange, 73%): IR (nujol): 2178, 2164 (N ≡ C), 841 (PF_6) cm^{-1}. Electronic spectrum (CH_2Cl_2): λ_{max} 283 (4.41), 247 (4.58) nm. ^1H NMR ($CDCl_3$): δ 2.11 (s, Me, 18H), 2.36 (b, CH_2), 2.90 (b, CH_2), 7.02–7.62 (m, Ph) ppm. $^{31}P\{^1H\}$ NMR ($CDCl_3$): δ 7.9 (s, 2P), −144.4 (sep. J_{PF} = 709 Hz) ppm. Anal. Calcd for $C_{54}H_{53}N_3F_{12}P_4Ni$: C, 56.18; H, 4.62; N, 3.64. Found: C, 56.00; H, 4.41; N, 3.33.

2.5. Preparation of $[NiCl(PPh_3)_2(XylNC)_2](PF_6)$ (5a)

Xylyl isocyanide (0.135 g, 1.03 mmol) and NH_4PF_6 (0.327 g, 0.50 mmol) in CH_2Cl_2 (20 cm^3) and acetone (20 cm^3) was added to $NiCl_2(PPh_3)_2$ (0.40 g, 0.76 mmol) in CH_2Cl_2 (15 cm^3)/acetone (5 cm^3) at room temperature. The work-up was carried out according to the procedure described in the preparation of **1a**. **5a** (reddish orange, 77%): IR (nujol): 2162 (N ≡ C), 841 (PF_6) cm^{-1}. Electronic spectrum (CH_2Cl_2): λ_{max} 408(sh), 345 (4.00), 258 (4.51) nm. ^1H NMR ($CDCl_3$): δ 1.73 (s, *o*-Me), 6.93–7.90 (m, Ph) ppm. $^{31}P\{^1H\}$ NMR ($CDCl_3$): δ 28.0 (s, PPh_3), −144.4 (sep, 710 Hz) ppm. Anal. Calcd for $C_{54}H_{48}N_2ClF_6P_3Ni$: C, 63.22; H, 4.71; N, 2.73. Found: C, 63.27; H, 4.71; N, 2.67.

The reddish orange bromide and reddish violet iodide complexes of triphenylphosphine were prepared according to the procedure described in the preparation of **1b**.

$[NiBr(PPh_3)_2(XylNC)_2](PF_6)$ · $3/2CH_2Cl_2$ (**5b**) · $3/2CH_2Cl_2$ (44%): IR (nujol): 2182, 2157 (N ≡ C), 837 (PF_6) cm^{-1}. Electronic spectrum (CH_2Cl_2): λ_{max} 437 (3.54), 341 (4.11), 284(sh), 260 (4.56) nm. ^1H NMR ($CDCl_3$): δ 1.75 (s, *o*-Me), 5.28 (s, CH_2Cl_2), 6.83–7.90 (m, Ph) ppm. $^{31}P\{^1H\}$ NMR ($CDCl_3$): δ 26.3 (s, PPh_3), −144.4 (sep, 710 Hz) ppm. Anal. Calcd for $C_{55.5}H_{51}N_2Cl_3BrF_6P_3Ni$: C, 55.64; H, 4.30; N, 2.34. Found: C, 56.28; H, 4.42; N, 2.30.

$[NiI(PPh_3)_2(XylNC)_2](PF_6)$ · $2CH_2Cl_2$ (**5c**) · $2CH_2Cl_2$ (72%): IR (nujol): 2180, 2157 (N ≡ C), 837 (PF_6) cm^{-1}. Electronic spectrum (CH_2Cl_2): λ_{max} 483 (3.34), 346 (4.20), 286(sh), 255 (4.64) nm. ^1H NMR ($CDCl_3$): δ 1.81 (s, *o*-Me), 5.28 (s, CH_2Cl_2), 6.80–7.90 (m, Ph) ppm. $^{31}P\{^1H\}$ NMR ($CDCl_3$): δ 25.2 (s, PPh_3), −144.4 (sep, 710 Hz) ppm. Anal. Calcd for $C_{56}H_{52}N_2Cl_4F_6IP_3Ni$: C, 52.25; H, 4.07; N, 2.18. Found: C, 52.57; H, 4.26; N, 2.15.

Table 1
Crystal data of **2a** · CH_2Cl_2, **3b** and **5a**

Compound	**2a** · CH_2Cl_2	**3b**	**5a**
Formula	$C_{46}H_{46}N_2F_6P_3Cl_3Ni$	$C_{56}H_{57}N_3P_4F_{12}Ni$	$C_{54}H_{48}N_2F_6P_3ClNi$
Mol. wt	998.85	1182.66	1026.05
Color	Reddish brown	Orange	Reddish brown
Cryst. dimen. (mm)	0.50 × 0.50 × 0.38	0.70 × 0.65 × 0.42	0.30 × 0.20 × 0.40
Cryst. syst.	Monoclinic	Monoclinic	Triclinic
Space group	$P2_1/c$ (No. 14)	*Pn* (No. 7)	P1 (No. 2)
Lattice parameters			
a (Å)	13.345(2)	12.763(3)	13.768(5)
b (Å)	10.984(2)	13.110(3)	17.23(1)
c (Å)	33.082(4)	17.114(3)	11.063(6)
a (°)	90.0	90.0	98.86(4)
β (°)	97.13(1)	102.55(2)	95.97(4)
γ (°)	90.0	90.0	75.48(3)
V (Å^3)	4812(3)	2795(2)	2504(2)
Z	4	2	2
D_{calcd} (g/cm^3)	1.379	1.405	1.361
μ (cm^{-1})	7.26	5.37	5.65
No. of unique data	4515 ($I > 4.0\sigma(I)$)	3298 ($I > 3.0\sigma(I)$)	2471 ($I > 3.0\sigma(I)$)
No. of variables	535	740	604
F(000)	2056	1220	1060
R; R_w[a]	0.064; 0.067	0.051; 0.038	0.063; 0.066
GOF	3.19	1.88	1.46

[a] $R = \Sigma||Fo| - |Fc||/|Fo|$ and $R_w = [\Sigma w(|Fo| - |Fc|)^2/\Sigma wFo^2]^{1/2}$ ($w = 1/\sigma^2(Fo)$).

2.6. Preparation of $[Ni(PPh_3)_2(XylNC)_3](PF_6)_2 \cdot CH_2Cl_2$ (6) $\cdot CH_2Cl_2$

Xylyl isocyanide (0.733 g, 5.59 mmol) and NH_4PF_6 (1.36 g, 8.32 mmol) in CH_2Cl_2 (20 cm^3) and acetone (20 cm^3) was added to $NiCl_2(PPh_3)_2$ (1.094 g, 1.67 mmol) in CH_2Cl_2 (15 cm^3)/acetone (5 cm^3) at room temperature. After stirred for 2 h, the solvent was removed and the residue was extracted with CH_2Cl_2, and followed by recrystallization from CH_2Cl_2-diethyl ether to give reddish brown crystals of the title compound (1.286 g, 57%): IR (nujol): 2155, 2126 (N ≡ C), 841 (PF_6) cm^{-1}. Electronic spectrum (CH_2Cl_2): λ_{max} 386 (3.86), 269(sh) nm. ^1H NMR ($CDCl_3$): δ 1.90 (s, *o*-Me), 5.30 (s, CH_2Cl_2), 6.93–7.90 (m, Ph) ppm. $^{31}P\{^1H\}$ NMR ($CDCl_3$): δ 46.3 (s, PPh_3), −144.4 (sep, 710 Hz) ppm. Anal. Calcd for $C_{64}H_{59}N_3Cl_2F_{12}P_4Ni$: C, 56.86; H, 4.40; N, 3.10. Found: C, 56.39; H, 4.21; N, 2.98.

2.7. Data collection

Complexes (**2a**, **3b**, and **5a**) were recrystallized from CH_2Cl_2/hexane or CH_2Cl_2/ether. Cell constants were determined on a Rigaku AFC5S four-circle automated diffractometer from the setting angles of 20–25 reflections in the range from $20.0° < 2\theta < 30.0°$. The crystal parameters along with data collection details are summarized in Table 1. Data collection was carried out on a Rigaku AFC5S diffractometer. Intensities were measured by the $2\theta - \omega$ scan method using MoKα radiation ($\lambda = 0.71069$ Å). A scan rate of 16° min^{-1} was used. Throughout the data collection, the intensities of the three standard reflections were measured every 150 reflections as a check of the stability of the crystals and no decay was observed.

A total 8957 independent intensities ($2\theta < 50°$) was measured for **2a**, 5163 ($2\theta < 50°$) for **3b**, and 8863 ($2\theta < 50°$) for **5a**. Of these, there are, respectively, 4515 ($I > 4.0\sigma(I)$), and 3298 ($I > 3.0\sigma(I)$), and 2471 ($I > 3.0\sigma(I)$) unique reflections which were used in the solutions and refinements of the structures. Intensities were corrected for Lorentz and polarization effects and for absorption. Atomic scattering factors and anomalous dispersion effects were taken from the usual tabulation [17]. All calculations were performed on a Digital VAX Station 3100 M38 computer using the TEXSAN-TEXRAY Program System [18].

2.8. Determination of the structures

The structures were solved by direct methods with MITHRIL. The nickel atom was located in the initial *E* map, and subsequent Fourier syntheses gave the positions of other non-hydrogen atoms. Hydrogen atoms were calculated at the ideal positions with the C–H

Table 2
Non-hydrogen positional parameters of $[NiCl(dppp)(XylNC)_2][PF_6]$ **2a** $\cdot CH_2Cl_2$

Atom	*x*	*y*	*z*
Ni(1)	0.79076(7)	0.0386(1)	0.16577(3)
Cl(1)	0.8832(2)	−0.1140(2)	0.20897(7)
Cl(2)	0.2536(6)	−0.0548(8)	0.0835(3)
Cl(3)	0.4175(4)	−0.0006(5)	0.0450(2)
P(1)	0.8967(2)	0.0651(2)	0.11960(6)!
P(2)	0.8615(2)	0.1917(2)	0.20191(6)!
P(3)	0.1991(2)	0.0971(3)	0.57689(9)
F(1)	0.1041(4)	0.0640(6)	0.5986(2)
F(2)	0.2200(5)	−0.0429(6)	0.5734(2)
F(3)	0.1320(7)	0.093(1)	0.5357(2)
F(4)	0.2945(5)	0.1305(7)	0.5564(2)
F(5)	0.1747(6)	0.2318(6)	0.5799(4)
F(6)	0.2679(5)	0.0896(8)	0.6181(2)
N(1)	0.6653(5)	−0.1420(6)	0.1133(2)
N(2)	0.5990(5)	0.0853(6)	0.2018(2)
C(1)	0.7171(6)	−0.0711(7)	0.1316(2)
C(2)	0.6753(6)	0.0684(7)	0.1896(2)
C(3)	0.5986(6)	−0.2326(7)	0.0966(3)
C(4)	0.6153(7)	−0.285(1)	0.0598(3)
C(5)	0.5489(9)	−0.375(1)	0.0444(3)
C(6)	0.4711(8)	−0.413(1)	0.0654(4)
C(7)	0.4567(8)	−0.359(1)	0.1010(4)
C(8)	0.5209(7)	−0.2673(9)	0.1177(3)
C(9)	0.5057(8)	−0.206(1)	0.1571(3)
C(10)	0.700(1)	−0.243(1)	0.0380(3)
C(11)	0.5024(7)	0.1083(9)	0.2133(3)
C(12)	0.4371(8)	0.173(1)	0.1860(4)
C(13)	0.3421(8)	0.198(1)	0.1981(4)
C(14)	0.3167(9)	0.159(1)	0.2340(5)
C(15)	0.383(1)	0.092(1)	0.2605(4)
C(16)	0.4803(8)	0.063(1)	0.2503(4)
C(17)	0.4645(8)	0.218(1)	0.1458(4)
C(18)	0.556(1)	−0.006(1)	0.2773(4)
C(19)	0.8275(6)	0.2008(8)	0.2533(2)
C(20)	0.8532(7)	0.1088(9)	0.2805(3)
C(21)	0.8338(8)	0.117(1)	0.3209(3)
C(22)	0.787(1)	0.218(1)	0.3335(3)
C(23)	0.760(1)	0.310(1)	0.3068(4)
C(24)	0.7790(8)	0.3041(9)	0.2669(3)
C(25)	0.8319(6)	0.3424(7)	0.1810(2)
C(26)	0.8910(6)	0.4412(8)	0.1949(3)
C(27)	0.8676(8)	0.5566(8)	0.1798(3)
C(28)	0.7866(8)	0.5723(8)	0.1503(3)
C(29)	0.7279(7)	0.476(1)	0.1360(3)
C(30)	0.7508(6)	0.3595(8)	0.1515(3)
C(31)	0.9985(6)	0.1845(7)	0.2091(2)
C(32)	1.0457(6)	0.2066(8)	0.1700(3)
C(33)	1.0256(6)	0.1035(8)	0.1393(3)
C(34)	0.8470(6)	0.1778(7)	0.0831(2)
C(35)	0.9053(7)	0.2747(9)	0.0713(3)
C(36)	0.864(1)	0.359(1)	0.0428(3)
C(37)	0.765(1)	0.349(1)	0.0264(3)
C(38)	0.7062(8)	0.254(1)	0.0376(3)
C(39)	0.7478(7)	0.1692(9)	0.0660(3)
C(41)	0.9476(7)	−0.1777(9)	0.1095(3)
C(42)	0.9788(8)	−0.277(1)	0.0875(3)
C(43)	0.9810(8)	−0.267(1)	0.0458(3)
C(44)	0.9546(8)	−0.158(1)	0.0259(3)
C(45)	0.9244(7)	−0.0608(9)	0.0479(3)
C(46)	0.9211(6)	−0.0681(7)	0.0895(2)
C(49)	0.265(2)	−0.014(3)	0.046(1)

Table 3
Non-hydrogen positional parameters of $[Ni(dppe)(MesNC)_2][PF_6]_2$ **3b**

Atom	x	y	z
Ni(1)	0	0.20968(8)	−0.0001
P(1)	−0.1651(2)	0.1620(2)	−0.0121(2)
P(2)	−0.0608(2)	0.3085(2)	−0.1058(1)
P(3)	0.8502(3)	0.8935(3)	0.7015(2)
P(4)	0.4900(3)	0.3842(2)	0.7359(2)
F(1)	0.9347(6)	0.9466(6)	0.6587(5)
F(2)	0.7704(6)	0.8412(6)	0.7463(5)
F(3)	0.8792(8)	0.7865(6)	0.6722(6)
F(4)	0.9386(6)	0.8800(8)	0.7755(5)
F(5)	0.818(1)	0.9957(7)	0.7288(7)
F(6)	0.7615(7)	0.9032(8)	0.6228(5)
F(7)	0.4122(6)	0.4440(5)	0.7785(4)
F(8)	0.4879(7)	0.4744(5)	0.6742(4)
F(9)	0.5889(7)	0.4412(6)	0.7922(5)
F(10)	0.5700(8)	0.3233(5)	0.6932(5)
F(11)	0.5057(9)	0.2981(6)	0.8004(5)
F(12)	0.3942(8)	0.3309(7)	0.6813(7)
N(1)	0.2081(6)	0.3320(6)	0.0280(4)
N(2)	0.1051(6)	0.0155(6)	−0.0641(5)
N(3)	0.0323(5)	0.1486(6)	0.1729(4)
C(1)	−0.1848(7)	0.0257(7)	0.0020(6)
C(2)	−0.1974(9)	−0.040(1)	−0.0627(7)
C(3)	−0.212(1)	−0.142(1)	−0.049(1)
C(4)	−0.214(1)	−0.177(1)	0.025(1)
C(5)	−0.201(1)	−0.111(1)	0.0896(7)
C(6)	−0.1866(8)	−0.0083(8)	0.0768(7)
C(7)	−0.2357(7)	0.2262(7)	0.0526(5)
C(8)	−0.1934(8)	0.3131(8)	0.0956(7)
C(9)	−0.249(1)	0.3636(8)	0.1441(7)
C(10)	−0.346(1)	0.327(1)	0.1520(7)
C(11)	−0.3910(8)	0.241(1)	0.1136(8)
C(12)	−0.3364(8)	0.1911(8)	0.0620(7)
C(13)	−0.0484(8)	0.4460(7)	−0.0957(6)
C(14)	−0.0339(8)	0.4943(8)	−0.0233(6)
C(15)	−0.031(1)	0.600(1)	−0.0191(8)
C(16)	−0.045(1)	0.6565(9)	−0.088(1)
C(17)	−0.063(1)	0.610(1)	−0.1634(9)
C(18)	−0.065(1)	0.505(1)	−0.1668(8)
C(19)	0.000(1)	0.2804(8)	−0.1878(6)
C(20)	−0.051(2)	0.215(1)	−0.2499(7)
C(21)	−0.001(2)	0.197(1)	−0.314(1)
C(22)	0.092(2)	0.238(2)	−0.315(1)
C(23)	0.143(1)	0.303(2)	−0.258(1)
C(24)	0.095(1)	0.323(1)	−0.1921(8)
C(25)	0.1294(7)	0.2891(7)	0.0198(5)
C(26)	0.3038(7)	0.3847(7)	0.0308(5)
C(27)	0.3744(8)	0.3490(7)	−0.0148(6)
C(28)	0.4646(7)	0.4044(8)	−0.0165(6)
C(29)	0.4860(8)	0.4959(9)	0.0275(7)
C(30)	0.415(1)	0.5262(8)	0.0736(7)
C(31)	0.3234(8)	0.4731(7)	0.0782(6)
C(32)	0.354(1)	0.2497(9)	−0.0590(8)
C(33)	0.248(1)	0.510(1)	0.1277(7)
C(34)	0.585(1)	0.557(1)	0.0234(9)
C(35)	0.0642(8)	0.0864(7)	−0.0457(6)
C(36)	0.1547(7)	−0.0753(7)	−0.0778(6)
C(37)	0.1613(8)	−0.1552(8)	−0.0212(6)
C(38)	0.207(1)	−0.2450(8)	−0.0381(7)
C(39)	0.2414(8)	−0.2618(7)	−0.1104(6)
C(40)	0.2341(8)	−0.1816(7)	−0.1626(6)
C(41)	0.1915(7)	−0.0863(7)	−0.1482(6)
C(42)	0.125(1)	−0.1387(8)	0.0552(7)
C(43)	0.184(1)	−0.0004(9)	−0.2067(7)
C(44)	0.281(1)	−0.3653(9)	−0.1282(7)
C(45)	0.0234(7)	0.1712(6)	0.1083(5)
C(46)	0.0305(7)	0.1267(7)	0.2528(5)
C(47)	0.0252(7)	0.0240(7)	0.2757(5)
C(48)	0.0089(8)	0.0048(7)	0.3524(6)
C(49)	0.0015(8)	0.083(1)	0.4055(6)
C(50)	0.0148(8)	0.1817(9)	0.3805(6)
C(51)	0.0297(8)	0.2066(8)	0.3054(6)
C(52)	0.045(1)	−0.0601(8)	0.2234(6)
C(53)	0.045(1)	0.3164(8)	0.2804(7)
C(54)	−0.024(1)	0.062(1)	0.4871(7)
C(55)	−0.2370(8)	0.191(1)	−0.1140(6)
C(56)	−0.2044(8)	0.289(1)	−0.1374(6)

distance of 0.95 Å, and were not refined. The non-hydrogen atoms were refined with anisotropic thermal parameters by using full-matrix least-squares methods. The final refinement converged to $R = 0.064$ and $R_w = 0.067$ for **2a**, 0.051 and 0.038 for **3b**, 0.063 and 0.066 for **5a**, respectively. Final difference Fourier syntheses showed peaks at heights up to 0.44–1.25 eA^{-3}. The positional parameters of complexes **2a**, **3b**, and **5a** are listed in Tables 2–4.

3. Results and discussion

3.1. Preparation of nickel(II) complexes

When a mixture of *cis*-$NiCl_2$(diphos) (diphos = $Ph_2P(CH_2)_nPPh_2$; dppe: $n = 2$; dppp: $n = 3$), xylyl isocyanide and NH_4PF_6 in ca. 1:2:1 ratio was treated at room temperature, a five-coordinate complex, formulated as $[NiCl(diphos)(XylNC)_2](PF_6)$ (**1a**: dppe; **2a**: dppp) was isolated in ca. 70% yield. Bromide and iodide complexes $[NiX(diphos)(XylNC)_2](PF_6)$ (**1b**: diphos = dppe, X = Br; **1c**: diphos = dppe, X = I; **2b**: diphos = dppp, X = Br; **2c**: diphos = dppp, X = I) were obtained by the metathesis reaction of **1a** or **2a** with potassium bromide or iodide in high yields (Scheme 1).

These complexes showed two bands in the range 2164–2182 cm^{-1} due to the terminal isocyanides. The absorption band of the longest wavelength in the electronic spectra is independent on the bite size of the chelating diphosphine ligands (vide infra), but red-shifted from ca. 390 nm to ca. 460 nm with the order of Cl, Br, and I, likely due to the increase of the HOMO energy with the decrease of electronegativity of halogens. The ^1H NMR spectra showed only one singlet at δ ca. 2.04–2.10 ppm for *o*-methyl protons. In the $^{31}P\{^1H\}$ NMR spectra, the signal appeared at δ ca. 70 ppm for the dppe complexes and at δ ca. 3 ppm for the

Table 4
Non-hydrogen positional parameters of $[NiCl(PPh_3)_2(XylNC)_2][PF_6]$ **5a**

Atom	x	y	z
Ni(1)	0.7744(1)	0.2075(1)	0.8619(2)
Cl(1)	0.8279(3)	0.1261(2)	1.0246(3)
P(1)	0.8702(3)	0.1183(2)	0.7267(3)
P(2)	0.6628(3)	0.3143(2)	0.9463(4)
P(3)	0.2499(8)	0.3405(4)	0.4512(7)
F(1)	0.140(1)	0.331(1)	0.428(2)
F(2)	0.360(1)	0.346(1)	0.462(2)
F(3)	0.282(2)	0.2545(9)	0.452(3)
F(4)	0.251(1)	0.330(2)	0.318(1)
F(5)	0.221(2)	0.425(1)	0.458(2)
F(6)	0.262(3)	0.344(2)	0.582(2)
N(1)	0.611(1)	0.1217(7)	0.779(1)
N(2)	0.9164(9)	0.3149(7)	0.873(1)
C(1)	0.671(1)	0.1570(8)	0.809(1)
C(2)	0.861(1)	0.2744(8)	0.869(1)
C(11)	0.544(1)	0.074(1)	0.746(2)
C(12)	0.549(2)	0.013(2)	0.811(2)
C(13)	0.477(2)	−0.031(2)	0.775(3)
C(14)	0.411(4)	−0.020(4)	0.685(5)
C(15)	0.412(2)	0.040(2)	0.618(4)
C(16)	0.477(2)	0.092(1)	0.645(2)
C(17)	0.622(2)	−0.003(2)	0.918(2)
C(18)	0.477(2)	0.159(2)	0.582(3)
C(21)	0.984(1)	0.3634(8)	0.871(1)
C(22)	1.050(1)	0.3717(9)	0.973(2)
C(23)	1.114(1)	0.420(1)	0.975(2)
C(24)	1.118(1)	0.457(1)	0.873(2)
C(25)	1.054(2)	0.446(1)	0.776(2)
C(26)	0.984(1)	0.400(1)	0.766(2)
C(27)	1.048(1)	0.330(1)	1.083(2)
C(28)	0.912(1)	0.389(1)	0.658(2)
C(31)	0.870(1)	0.0131(8)	0.728(1)
C(32)	0.793(1)	−0.017(1)	0.663(1)
C(33)	0.792(1)	−0.096(1)	0.662(2)
C(34)	0.864(1)	−0.147(1)	0.724(2)
C(35)	0.940(1)	−0.117(1)	0.791(1)
C(36)	0.944(1)	−0.039(1)	0.792(1)
C(41)	1.000(1)	0.1262(8)	0.746(1)
C(42)	1.048(1)	0.148(1)	0.658(2)
C(43)	1.144(2)	0.159(1)	0.682(2)
C(44)	1.195(1)	0.149(1)	0.796(2)
C(45)	1.150(1)	0.128(1)	0.882(2)
C(46)	1.052(1)	0.1179(9)	0.862(2)
C(51)	0.830(1)	0.1372(9)	0.572(1)
C(52)	0.857(1)	0.0773(9)	0.471(1)
C(53)	0.827(1)	0.095(1)	0.355(1)
C(54)	0.766(1)	0.170(1)	0.335(2)
C(55)	0.739(1)	0.228(1)	0.430(1)
C(56)	0.771(1)	0.210(1)	0.548(1)
C(61)	0.635(1)	0.3884(9)	0.840(1)
C(62)	0.598(1)	0.3686(9)	0.721(2)
C(63)	0.583(1)	0.419(1)	0.634(2)
C(64)	0.604(2)	0.493(1)	0.667(2)
C(65)	0.642(2)	0.516(1)	0.780(2)
C(66)	0.657(1)	0.463(1)	0.869(2)
C(71)	0.542(1)	0.299(1)	0.975(2)
C(72)	0.539(1)	0.262(1)	1.072(2)
C(73)	0.449(2)	0.248(1)	1.103(2)
C(74)	0.366(2)	0.266(1)	1.030(3)
C(75)	0.371(2)	0.301(1)	0.930(2)
C(76)	0.456(1)	0.319(1)	0.901(2)
C(81)	0.702(1)	0.3632(8)	1.094(1)
C(82)	0.640(1)	0.4326(9)	1.152(2)
C(83)	0.669(1)	0.465(1)	1.265(2)
C(84)	0.761(2)	0.433(1)	1.319(1)
C(85)	0.823(1)	0.363(1)	1.267(2)
C(86)	0.793(1)	0.3287(8)	1.150(1)

dppp complexes. The similar behaviors have been noted in the nickel(II) and palladium(II) complexes, $[M(diphos)_2](BF_4)_2$ (diphos = dppe, dppp); δ 52–55 ppm for the dppe complexes and δ −0.8–0 ppm for the dppp ones [19]. The chemical shifts of P atoms are independent on halogens.

When a similar reaction of *cis*-$NiCl_2$(diphos) with three molar amount of xylyl isocyanide was carried out in the presence of excess NH_4PF_6, one more Cl atom was replaced with xylyl isocyanide to give $[Ni(diphos)(XylNC)_3](PF_6)_2$ (**3**: dppe; **4**: dppp) as orange crystals. A mesityl isocyanide complex, $[Ni(dppe)(MesNC)_3](PF_6)_2$ (**3b**) was obtained in a similar manner. The infrared spectra showed three bands for terminal isocyanide ligands. The $^{31}P\{^1H\}$ NMR spectrum appeared at the lower field by ca. 4–10 ppm than those of complexes **1** and **2**, responsible for the higher π back-bonding ability of isocyanide than that of the Cl atom. Stereochemistry for five-coordinate complexes is either square-pyramidal (*spy*) or trigonal-bipyramidal (*tbp*).

Since the $^{31}P\{^1H\}$ NMR spectra showed only one signal for all complexes, two possible structures are expected; diphosphine ligand is located either at two sites of the basal plane for the *tbp* form (a C_{2v} symmetry) or at two sites of the square plane for the *spy* one (a C_s symmetry), as depicted in Fig. 1. Two $\upsilon(N \equiv C)$ bands were expected for **1** and **2** and three bands for **3** and **4** in the infrared spectra, based on the molecular symmetry. It was difficult to confirm from the results of the infrared spectra whether complexes is a *spy* or *tbp* form.

For nickel complexes containing diphosphine ligands with methylene, ethylene, and trimethylene linkages, the P–M–P bite angles formed by the chelating ligand are approximately 73° [19], 85° [20–23], and 90° [24], respectively. If the complex adopts a *tbp* form, the P–Ni–P angles would be 85–90° from the results of the

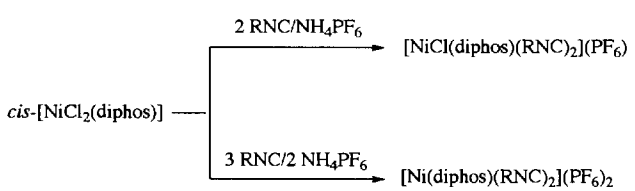

Scheme 1. Reactions of $[NiCl_2(diphos)]$ with isocyanide and NH_4PF_6, where diphos = dppe and dppp.

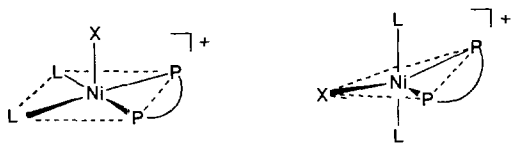

Fig. 1. Possible structures of $[NiX(diphos)(RNC)_2]^+$.

bite angles found in the literatures, and are narrower than those of the ideal angle. The *tbp* complexes with small angles were found in $Rh(P^iBu_3)_2ClH_2$ [25], $Ir(\eta^3\text{-PNP})(Me)(neo\text{-Pe})$ (neo-Pe = neopentyl, PNP = $(Ph_2PCH_2Me_2Si)_2N$) [26], $Ir(P^iPr_3)_2Cl(Ph)H$ [27], $Rh(P^iPr_3)_2ClH_2$ [28], and $Rh(P^iPr_3)_2ClX[C(O)Ph]$ (X = H, Cl) [29]; all reveal surprisingly small R–M–R′ angles (65°–85°) and have the phosphine ligands at the apical positions.

We assumed that the square-pyramidal structure (A) is superior to the trigonal-bipyramidal one (B), because of releasing from great distortion resulted in the unusual *tbp* structure and of no complexes that two phosphine ligands occupied at the basal sites. However, the ^1H NMR spectra of complexes **3** and **4** showed only one singlet for the *o*-methyl groups of isocyanides, incompatible with the proposed structure. In an attempt to exclude this dilemma, the X-ray analyses of **2a** and **3b** were carried out, and supported the proposed structure (A) (Figs. 2 and 3) (vide infra). Only one singlet for complexes **3** and **4** is likely due to an accidental degeneracy or the rapid ligand exchange.

Treatment of $NiCl_2(PPh_3)_2$ with xylyl isocyanide in the presence of a half-equivalent NH_4PF_6 gave reddish brown crystals **5a** formulated as $[NiCl(PPh_3)_2(XylNC)_2](PF_6)$ (Scheme 2). Bromide and iodide complex **5b** and **5c** were prepared by the metathesis of **5a** with KBr or KI, respectively. When $NiCl_2(PPh_3)_2$ was treated with an excess of xylyl isocyanide and NH_4PF_6, the further substitution reaction occurred to give reddish brown complex $[Ni(PPh_3)_2(XylNC)_3](PF_6)_2$ **6**. Complex **6** was also prepared by the reaction of **5a** with xylyl isocyanide in the presence of NH_4PF_6. The $^{31}P\{^1H\}$ NMR spectra showed a singlet at δ ca. 26 ppm for **5** and at δ 46.3 ppm for **6**, respectively. These complexes are suggested as the square-pyramidal geometry on the basis of similarity to the structures of **1**–**4**, and the basal plane is assumed to take a *trans*-form from steric demand. An X-ray analysis of **5a** confirmed the proposed structure (Fig. 4) (vide

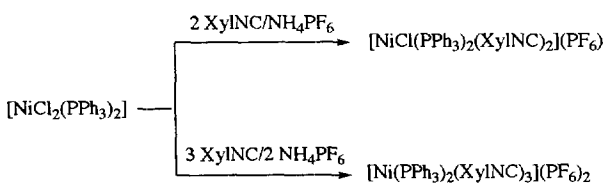

Scheme 2. Reactions of $[NiCl_2(PPh_3)_2]$ with xylyl isocyanide and NH_4PF_6.

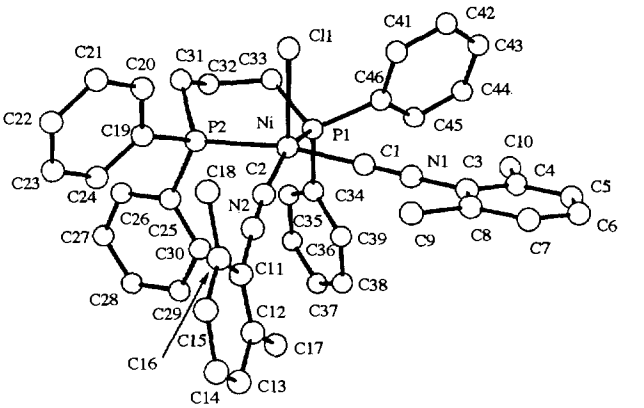

Fig. 2. Structure of $[NiCl(dppp)(XylNC)_2](PF_6)$ **2a**. The PF_6 anion and hydrogen atoms are omitted for clarity.

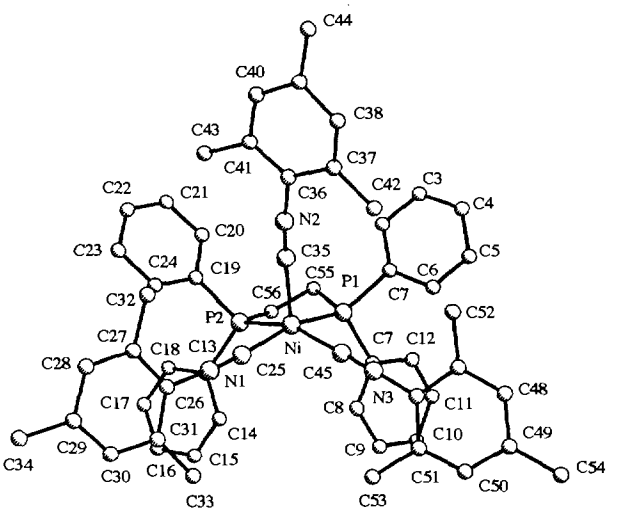

Fig. 3. Structure of $[Ni(dppe)(MesNC)_3][PF_6)_2$ **3b**. The PF_6 anions and hydrogen atoms are omitted for clarity.

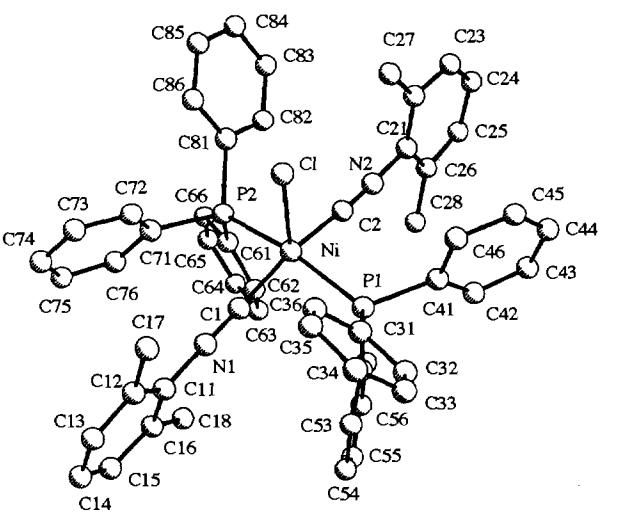

Fig. 4. Structure of $[NiCl(PPh_3)_2(XylNC)_2](PF_6)$ **5a**. The PF_6 anion and hydrogen atoms are omitted for clarity.

Table 5
Selected bond lengths and angles of $[NiCl(dppp)(XylNC)_2](PF_6)\cdot CH_2Cl_2$ **1a**$\cdot CH_2Cl_2$

Bond lengths (Å)			
Ni–Cl(1)	2.437(2)	Ni–P(1)	2.225(2)
Ni–P(2)	2.207(2)	Ni–C(1)	1.849(8)
Ni–C(2)	1.845(8)	C(1)–N(1)	1.161(9)
C(2)–N(2)	1.156(8)		
Bond angles (°)			
Cl–Ni–P(1)	100.03(9)	Cl–Ni–P(2)	93.16(8)
Cl–Ni–C(1)	95.9(2)	Cl–Ni–C(2)	105.1(3)
P(1)–Ni–P(2)	90.36(8)	P(1)–Ni–C(1)	90.0(2)
P(1)–Ni–C(2)	154.9(3)	P(2)–Ni–C(1)	170.7(2)
P(2)–Ni–C(2)	87.5(3)	C(1)–Ni–C(2)	88.2(3)
Ni–C(1)–N(1)	173.2(7)	C(1)–N(1)–C(3)	171.8(8)
Ni–C(2)–N(2)	175.0(7)	C(2)–N(2)–C(11)	175.2(9)

Table 7
Selected bond lengths and angles of $[NiCl(PPh_3)_2(XylNC)_2](PF_6)_2$ **5a**

Bond lengths (Å)			
Ni–Cl	2.395(4)	Ni–P(1)	2.241(4)
Ni–P(2)	2.229(5)	Ni–C(1)	1.84(1)
Ni–C(2)	1.84(2)	C(1)–N(1)	1.14(2)
C(2)–N(2)	1.15(2)		
Bond angles (°)			
Cl–Ni–P(1)	93.6(2)	Cl–Ni–P(2)	103.5(2)
Cl–Ni–C(1)	91.4(4)	Cl–Ni–C(2)	107.5(4)
P(1)–Ni–P(2)	162.8(2)	P(1)–Ni–C(1)	88.4(4)
P(1)–Ni–C(2)	89.2(4)	P(2)–Ni–C(1)	89.3(4)
P(2)–Ni–C(2)	87.5(4)	C(1)–Ni–C(2)	161.1(6)
Ni–C(1)–N(1)	176(1)	C(1)–N(1)–C(11)	176(2)
Ni–C(2)–N(2)	179(1)	C(2)–N(2)–C(21)	177(1)

infra). Since the complexes **5** and **6** have the C_{2v} symmetry, the numbers of ν(NC) bonds are usually expected to be two for **5** and three for **6**, respectively. However, the infrared spectra of **5** and **6** showed only one peak at ca. 2160 cm^{-1} due to the terminal isocyanide, probably due to an accidental degeneracy.

3.2. X-ray structures of 2a · CH_2Cl_2, 3b, and 5a

The selected bond lengths and angles are listed in Tables 5–8. Complexes (**2a**, **3b** and **5a**) are distorted square-pyramidal as expected and the basal plane of **5a** with monophosphine ligands has a *trans*-configuration. The Cl atom in **2a** and **3b** and the terminal carbon atom of isocyanide in **5a** are occupied at the apical site.

The average Cl–Ni–P angle is more narrow than that of the Cl–Ni–C angles; the formers are 97° for **2a** and 99° for **3b**, whereas the latters are 101° for **2a**, and 100° for **3b**, respectively. However, the result was opposite for complex **5a**; the average C35–Ni–P angle is 103° and the C35–Ni–C (basal plane) angle is 98°. Each Ni atom is located slightly above the PPCC plane. The one phenyl ring of two or three P-bonded phenyl groups is occupied toward the vacant side of the *spy* configuration. It minimized the steric repulsion between phenyl groups at the phosphine ligands. The torsion angles of the C1–N1–C3–C8 and C2–N2–C11–C16 in **2a** are 24° and 167°, and those of the corresponding C1–N1–C11–C12 and C2–N2–C21–C22 in **3b** are 32° and −153°, respectively. These also minimizes the steric repulsion with neighbouring phosphine ligands. The Ni–C–N and C–N–C angles of each complex are not different from the usual value.

In the complex **2a** the six-membered ring formed by the chelating diphos-ligand consists of a chair-form. The bite angles in **2a** are 90.36(8)° and that in **3b**, 86.0(1)°. These values are in good agreement with usual angles found in the dppp and dppe complexes of nickel. The Ni–P and Ni–C bond lengths in the basal plane of **2a** and **3b** are not significantly different and are normal with the average values of 2.22 and 1.85 Å, respectively. However, in the complex **5a** the Ni–P1 bond distance of 2.165(3) Å in the basal plane is significantly shorter than the Ni–P2 one of 2.224(3) Å, but each Ni–C bond distance at their *trans*-positions is not sig-

Table 6
Selected bond lengths and angles of $[Ni(dppe)(MesNC)_3](PF_6)_2$ **3b**

Bond lengths (Å)			
Ni–P(1)	2.165(3)	Ni–P(2)	2.224(3)
Ni–C(25)	1.92(1)	Ni–C(35)	2.04(1)
Ni–C(45)	1.883(9)	C(25)–N(1)	1.13(1)
C(35)–N(1)	1.14(1)	C(45)–N(3)	1.13(1)
Bond angles (°)			
P(1)–Ni–P(2)	86.0(1)	P(1)–Ni–C(25)	162.9(3)
P(1)–Ni–C(35)	101.5(3)	P(1)–Ni–C(45)	87.6(3)
P(2)–Ni–C(25)	87.9(3)	P(2)–Ni–C(35)	104.4(3)
P(2)–Ni–C(45)	155.6(3)	C(25)–Ni–C(35)	95.5(4)
C(25)–Ni–C(45)	91.4(4)	C(35)–Ni–C(45)	100.0(4)
Ni(1)–C(25)–N(1)	175.5(8)	C(25)–N(1)–C(26)	175.0(9)
Ni(1)–C(35)–N(2)	173.6(9)	C(35)–N(2)–C(36)	173(1)
Ni(1)–C(45)–N(3)	176.7(8)	C(45)–N(3)–C(46)	172.5(9)

Table 8
Comparison of the selected bond lengths and angles

	1a$\cdot CH_2Cl_2$	**3b**	**5a**
Ni–P[a]	2.216	2.194	2.236
Ni–Cl	2.437	–	2.395
Ni–C[a]	1.847	1.948	1.84
P–Ni–P	90.4	86.0	162.8
P–Ni–Cl[a]	96.6	–	98.6
P–Ni–C[a]	88.8	87.8	88.6
		103.0[b]	
	162.8	159.3	
Cl–Ni–C[a]	100.5	–	99.4
C–Ni–C	88.2	95.6[a]	161.2

[a]Average value.
[b]P–Ni–C (apical) bond angle.

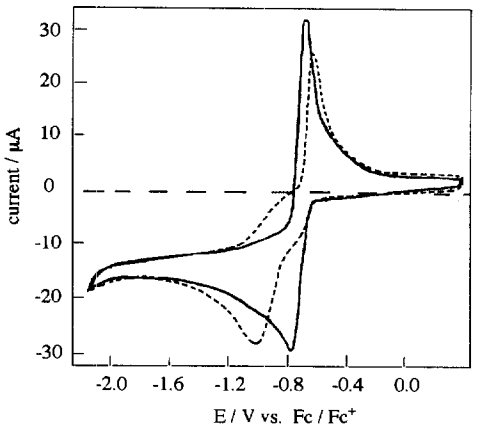

Fig. 5. Cyclic voltammograms of **2a** and **2a**/xylyl isocyanide (a 1:10 ratio).

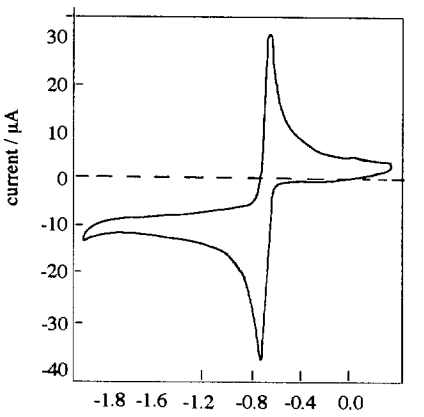

Fig. 6. Cyclic voltammogram of **3a**.

nificantly different. Since no unusual contact between dppe and isocyanide ligands was observed, it may be likely due to packing force. The Ni–P bond length in the basal plane among three complexes is longer in the order **3b** < **2a** < **5a** and this order was traced back to the Ni–C length, where bond distance decreased in the opposite order **3b** > **2a** ~ **5a**.

The Ni-apical C35 bond length is 2.04(1) Å, being longer than the average distance of 1.90 Å in the basal plane, minimizing steric repulsion to neighbouring ligands. The Ni–Cl bond length (2.437(2) Å) in **2a** is longer than that (2.395(4) Å) of **5a**, suggesting that steric bulkiness of **2a** with the bidentate ligand is greater than that of **5a** with two monodentate ligands.

3.3. Electrochemical reaction

Electrochemical data of complexes are shown in Table 9. Fig. 5 shows the cyclic voltammograms (CVs) of **1a** and a mixture of **1a** and xylyl isocyanide at a 1:10 ratio in a MeCN–CH_2Cl_2 (9:1) solution, using [$^nBu_4N$][ClO_4]) as a supporting electrolyte. The $E_{1/2}$ value of **1a** is −0.88 V, where the E_{pa} and E_{pc} values are −0.685 V and −1.072 V, respectively. The CV is quasi-reversible and the potential separations between anodic and cathodic peaks become narrower with increase of sweep rates. For sweep rates between 0.01 and 0.20 V s^{-1} the ratio $i_{pc}/r^{1/2}$ was constant and the s_{pa}/i_{pc} ratio is in the range of 0.9–1.1, in accord with diffusion control. The electrochemical reaction of the complex **1a** proceeded with two-electrons redox reaction in comparison with the results of the electroreduction of [$NiI_2(RNC)_2$] and [$Ni(RNC)_4$]$^{2+}$ [11,12], and consumption of 2 F (96.5 × 2 kC) of charge per mole of complex.

The CV of **3a** appeared at −0.69 V for $E_{1/2}$ (at −0.664 V for E_{pa} and −0.723 V for E_{pc}) with i_{pa}/i_{pc} = 1.0, also being a quasi-reversible and two-electrons transfer reaction (Fig. 6 and Scheme 3). Redox wave appeared in more positive region than that of the complex **1a**, because of higher π-acceptor ability of the

Table 9
Redox potentials of the five-coordinated complexes[a]

Compound		Without RNC			With RNC (10 eq.)		
		$E_{1/2}$	ΔE	i_{pa}/i_{pc}	$E_{1/2}$	ΔE	i_{pa}/i_{pc}
[NiCl(dppe)(XylNC)$_2$]$^+$	**1a**	−0.88	0.39	1.1	−0.74	0.08	1.1
[NiBr(dppe)(XylNC)$_2$]$^+$	**1b**	−0.86	0.38	0.9	−0.75	0.08	1.1
[NiI(dppe)(XylNC)$_2$]$^+$	**1c**	−0.79	0.26	1.0	−0.75	0.09	1.3
[NiCl(dppp)(XylNC)$_2$]$^+$	**2a**	−0.89	0.50	0.9	−0.70	0.04	1.1
[NiBr(dppp)(XylNC)$_2$]$^+$	**2b**	−0.89	0.51	1.0	−0.70	0.04	1.2
[NiI(dppp)(XylNC)$_2$]$^+$	**2c**	−0.83	0.38	1.0	−0.73	0.14	1.5
[Ni(dppe)(XylNC)$_3$]$^{2+}$	**3a**	−0.69	0.06	1.1	−0.67	0.07	1.0
[Ni(dppp)(XylNC)$_3$]$^{2+}$	**4**	−0.65	0.06	0.9	−0.65	0.07	1.0
[NiCl(PPh$_3$)$_2$(XylNC)$_2$]$^+$	**5a**	−0.68	0.34	0.9	−0.48	0.04	1.1
[NiBr(PPh$_3$)$_2$(XylNC)$_2$]$^+$	**5b**	−0.68	0.28	1.1	−0.50	0.05	1.0
[NiCl(PPh$_3$)$_2$(XylNC)$_2$]$^+$	**5c**	−0.65	0.14	1.0	−0.50	0.04	1.0
[Ni(PPh$_3$)$_2$(XylNC)$_3$]$^{2+}$	**6**	−0.49	0.06	1.0	0.49	0.06	1.1

[a]A sample (ca. 1.0 mM) was measured in a 0.1 M MeCN–CH_2Cl_2 (9:1) solution containing [n-Bu_4N][ClO_4]. The Fc/Fc^+ couple was used as a reference, where Fc is ferrocene.

isocyanide ligand than the halogen atom. The $E_{1/2}$ potential of **3a** was kept unchanged in the presence of excess xylyl isocyanide, showing no dissociation of isocyanide or other ligand. The half-wave potential of **3a** by the dropping mercury electrode (DME) appeared at -0.70 V, showing the absence of an interaction between mercury and **3a**, in which such interaction has been observed in the electrochemical reaction of neutral complexes $NiX_2(RNC)_2$ by the DME [11,12].

Since the complex **1a** readily reacted with xylyl isocyanide in the presence of NH_4PF_6 to give **3a**, the CV of a mixture of **1a** and excess xylyl isocyanide is expected to show the $E_{1/2}$ value similar to that of **3a**. The redox potentials of **1a** shifted more positive and the ΔE values become narrower with addition of 2,6-xylyl isocyanide. Finally, the $E_{1/2}$ potential appeared at -0.79 V (-0.736 V for E_{pa} and -0.824 V for E_{pc}), being out of accord with that of **3a**. This suggests that there exists an equilibrium between **1a** and **3a** (Scheme 2). In fact, the $E_{1/2}$ potential was in accord with that of **1a** by addition of $^nBu_4NCl$ to this solution. The half-wave potential of the mixture by the DME appeared at -0.77 V, also suggesting the absence of the interactions. Similar electrochemical behaviors were also observed in bromide and iodide complexes (**1b** and **1c**). The addition of dppe to **1** or **3a** did not lead to shift of the half-wave potential.

The redox couple of the dppp complex **2a** appeared at $E_{pa} = -0.640$ V and $E_{pc} = -1.139$ V with $E_{1/2} = -0.89$ V, and did not significantly change even by the addition of xylyl isocyanide or dppp to this solution. These results suggest that the reactions of **2a** with added ligands do not occur. The bromide and iodide complexes (**2b** and **2c**) showed the analogous result to **2a**. There is the absence of replacement or dissociation of ligands in each complex. Complexes containing a six-membered ring prevent dissociation of ligands and are assumed to be more stable than the five-membered ring compounds, because of releasing of ring strain in comparison to a five-membered ring.

The CVs of triphenylphosphine complexes **5** are also quasi-reversibe. The $E_{1/2}$ potentials appeared at -0.67, -0.68 and -0.60 V for **5a**, **5b** and **5c**, respectively, and the i_{pa}/i_{pc} values are near unity. Addition of xylyl isocyanide to these complexes finally led to the $E_{1/2}$ potential of -0.50 V. This value was in good accord

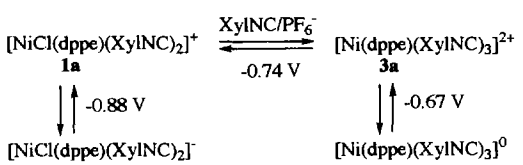

Scheme 3. Electrochemical reactions of **1a** and **3a**.

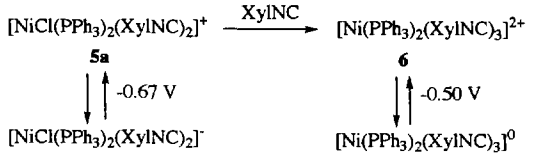

Scheme 4. Electrochemical reactions of **5a** and **6**.

with that of the complex **6**, showing that a complete conversion from **5a** to **6** occurred (Scheme 4). The CV of a mixture of **5a** (or **6**) and PPh_3 showed a pattern similar to those of the corresponding original complexes. There were no effects for added phosphine ligand.

References

[1] Y. Yamamoto, K. Takahashi, H. Yamazaki, Chem. Lett. (1985) 201.
[2] Y. Yamamoto, K. Takahashi, H. Yamazaki, J. Am. Chem. Soc. 109 (1986) 2458.
[3] Y. Yamamoto, K. Takahashi, H. Yamazaki, J. Chem. Soc., Dalton Trans. (1987) 1833.
[4] Y. Yamamoto, K. Takahashi, H. Yamazaki, Bull. Chem. Soc. Jpn. 60 (1987) 2665.
[5] K. Takahashi, Y. Yamamoto, K. Matsuda, H. Yamazaki, Electrochim. Acta 33 (1988) 1489.
[6] Y. Yamamoto, H. Yamazaki, Organometallics 12 (1993) 933.
[7] T. Tanase, K. Kawahara, H. Ukaji, K. Kobayashi, H. Yamazaki, Y. Yamamoto, Inorg. Chem. 32 (1993) 3682.
[8] T. Tanase, H. Ukaji, Y. Kudo, M. Ohno, K. Kobayashi, Y. Yamamoto, Organometallics 13 (1994) 1374.
[9] T. Tanase, Y. Yamamoto, R.J. Puddephatt, Organometallics 15 (1996) 1502.
[10] Y. Yamamoto, T. Tanase, H. Ukaji, T. Igoshi, J. Organomet. Chem. 498 (1995) C23.
[11] K. Ehara, K. Kumagai, Y. Yamamoto, K. Takahashi, H. Yamazaki, J. Organomet. Chem. 410 (1990) C49.
[12] Y. Yamamoto, K. Ehara, K. Takahashi, Bull. Chem. Soc. Jpn. 66 (1993) 778.
[13] I. Ugi, R. Meyer, Chetn. Ber. 93 (1960) 239.
[14] R. Busby, M.B. Hursthouse, P.S. Jarrett, C.W. Lehmann, K.M.A. Malik, C. Phillips, J. Chem. Soc., Dalton Trans. (1993) 3767.
[15] G.R. van Hecke, W.D. Harrocks Jr., Inorg. Chem. 5 (1966) 1969.
[16] G. Booth, J. Chatt, J. Chem. Soc. (1965) 3238.
[17] D.T. Cromer, J.T. Waber, International Tables for X-ray Crystallography, vol. 4, Kynoch Press, Birmingham, UK, 1974, Table 2.2A.
[18] TEXSAN-TEXRAY, Structure Analysis Package, Molecular Structure, 1985.
[19] A. Miedaner, R.C. Haltiwanger, D.L. Dubois, Inorg. Chem. 30 (1991) 417.
[20] W.H. Hohman, D.J. Kountz, D.W. Meek, Inorg. Chem. 25 (1986) 616.
[21] V.M. Di, J. Chem. Soc., Dalton Trans. (1975) 2360.
[22] S.A. Laneman, G.G. Stanley, Inorg. Chem. 26 (1987) 1177.
[23] A. Orlandini, L. Sacconi, Inorg. Chem. 15 (1976) 78.
[24] R. Mason, G.R. Scollary, D.L. DuBois, D.W. Meek, J. Organomet. Chem. 144 (1976) C30.

[25] T. Yoshida, S. Otsuka, M. Matsumoto, K. Nakatsu, Inorg. Chim. Acta 29 (1978) L257.
[26] M.D. Fryzuk, P.A. MacNeil, R.G. Ball, J. Am. Chem. Soc. 108 (1986) 6414.
[27] H. Werner, A. Holm, M. Dziallas, Angew. Chem., Int. Ed. Engl. 25 (1986) 1090.
[28] R.L. Harlow, D.L. Thorn, R.T. Baker, N.L. Jones, Inorg. Chem. 31 (1992) 993.
[29] K. Wang, T.J. Emge, A.S. Goldman, C. Li, S.P. Nolan, Organometallics 14 (1995) 4929.